Astron. Astrophys. 336, 281–289 (1998)

ASTRONOMY AND ASTROPHYSICS

Building reliable models of M dwarf chromospheres: the impact of the usual assumptions

Ambretta Falchi[1] **and Pablo J.D. Mauas**[2]

[1] Osservatorio Astrofisico di Arcetri, Largo E. Fermi 5, I-50155 Firenze, Italy
[2] Instituto de Astronomía y Física del Espacio, CC 67, Suc. 28, 1428-Buenos Aires, R. Argentina

Received 23 December 1997 / Accepted 19 May 1998

Abstract. We study different approximations usually made to simplify the calculation of chromospheric models of M dwarf stars. The approximations we discuss in details are: the assumption that the minority species are in LTE, the omission of the contribution of numerous atomic and molecular lines (*line blanketing*) to the opacity, and the Complete Frequency Redistribution for the Ly$_\alpha$ line.

We consider a "cold" chromospheric model corresponding to a low activity dM star and a "hot" one corresponding to a very active dMe star. We find that the assumptions under study affect more strongly the cold than the hot model. In particular the approximation of Complete Frequency Redistribution in the Ly$_\alpha$ line, through the statistical equilibrium and ionization equilibrium equation, changes the electron density in the high chromosphere and strongly affects other line profiles.

Key words: stars: atmospheres – stars: chromosphere – stars: late-type

1. Introduction

Different grids of atmospheric models have been constructed for dM stars, as a way to understand the wide range of emission levels in the observed spectra (Cram & Mullan, 1979, Giampapa et al., 1982). For different T vs. z distributions, the non-LTE populations for hydrogen are computed, solving simultaneously the equations of hydrostatic equilibrium, radiative transfer, and statistical equilibrium. Once the models are completed, the emerging profiles for some chromospheric lines, usually H$_\alpha$ or Ca II K, are computed. In this way, constraints on the structure of the stellar chromosphere are found from the observed spectrum.

A very thorough work of this kind has been done by the Armagh group (Houdebine & Doyle, 1994a; Houdebine et al. 1995; Houdebine et al. 1996), who constructed a grid of chromospheric models of early M dwarfs of different activity levels, to investigate the response of the Hydrogen spectrum to different atmospheric parameters. This grid has been used by Houdebine and Doyle (1994b) for modeling Au Mic (dM2.5e). Andretta et al. (1997) explored the dependence on chromospheric activity of the Na I D lines and found that these lines are a good diagnostic for the lower-middle chromosphere to be used together with H I lines.

A different approach, thoroughly used in the Sun, has been to construct semiempirical chromospheric models for particular stars. By semiempirical we mean that the model is computed to match a certain number of spectral features as well as possible. For a given model, the computed spectrum is compared with the observations. The assumed T vs z distribution is modified, until a satisfactory match between the observations and the calculations is obtained. This approach has been used, for example, by Thatcher et al. (1991), who constructed a model for the dK2 star ϵ Eridani, and by Luttermoser et al. (1994) for the M6 III star 30 g Her.

Using this approach, we computed a chromospheric model of AD Leo, an active dM3.5 star, in its quiescent state (Mauas & Falchi 1994, Paper I) and during a large flare (Mauas & Falchi 1996, Paper II). We also constructed chromospheric models of Gl 588 and Gl 628 (dM 3-4) that are considered very low-activity stars (Mauas et al. 1997, Paper III). A comparison between the chromospheric models of stars of the same spectral type but different levels of activity allowed us to constrain the heating necessary to sustain the hotter chromosphere. The features we used to construct the models were the continuum between 3500 and 9000 Å, the four highest Balmer lines, the Ca II K line, the Na D lines, and the Ly$_\alpha$ flux.

As can be seen, a common point between this two approaches to chromospheric modelling is that a large number of models has to be constructed, either to build a complete grid, or to attain a good match between computed and observed profiles.

To simplify the computations, several approximations are usually made in the way the problem is treated. However, before any conclusions on the atmospheric structure are drawn from the models, it is necessary to assess the importance of the approximations used in the computations. As part of our ongoing project of constructing chromospheric models for cool dwarf stars, we study how some of these approximations affect the emergent spectrum.

In Sect. 2 we explain how the models are built. In Sect. 3 we discuss some usual approximations made in the literature and we show the effect on the emergent spectrum for two at-

Send offprint requests to: A. Falchi

mospheric models representing stars of very different levels of stellar activity. Finally, in Sect. 4 we discuss the results.

2. Model construction

For our models we assume a plane-parallel geometry, as usual for dwarf stars, since the thickness of the atmosphere is small compared to the radius of the star. We also assume a homogeneous (1-D) atmosphere, which is probably a good approximation for inactive stars, especially those usually considered as "basal" stars, while it may be less adequate for active stars (e.g. Robinson et al. 1990, Houdebine & Doyle 1994b, Paper I). In any case, we believe that the results obtained in our previous work justify *a posteriori* this approximation.

The modelling was done using the program Pandora developed, and kindly provided, by Dr. E. H. Avrett (see Avrett & Loser 1984). Given a T vs. z distribution, we solved the non-LTE radiative transfer, statistical and hydrostatic equilibrium equations, and self-consistently compute non-LTE populations for 8 levels of H, 13 levels of He I, 9 levels of C I, 15 levels of Fe I, 8 levels of Si I, Ca I and Na I, 6 levels of Al I, and 7 levels of Mg I. In addition, we also computed 6 levels of He II and Mg II, and 5 of Ca II. For every species under consideration, we solve the equations of statistical equilibrium and of radiative transfer, including all the bound-free transitions and the most important bound-bound transitions. This amounted to a total of 99 b-f and 143 b-b transitions. For hydrogen, we also tested a 15 level atomic model, computing all its 15 b-f and 105 b-b transitions, and found no significative difference in the emitted spectra.

For each b-f transition we assumed that the absorption coefficient has a Voigt profile, given by

$$\phi_\nu = \frac{a}{\pi^{3/2}\Delta\nu_{\rm D}} \int_{-\infty}^{\infty} \frac{e^{-x^2}dx}{a^2 + (x - (\nu-\nu_0)/\Delta\nu_{\rm D})^2} \qquad (1)$$

where $\Delta\nu_{\rm D}$ is the Doppler width, and *a* is the Voigt parameter

$$a = \frac{C_{\rm rad} + C_{\rm VdW}\left(\frac{n_{\rm HI}}{10^{16}}\right)\left(\frac{T}{5000}\right)^{0.3} + C_{\rm Stk}\left(\frac{n_e}{10^{12}}\right)}{\Delta\lambda_{\rm D}} \; . \qquad (2)$$

Here $n_{\rm HI}$ and n_e are the atomic hydrogen and electron densities, T is the electron temperature, and the Doppler width $\Delta\lambda_{\rm D} = (\lambda/\nu)\Delta\nu_{\rm D}$ is in Å units. In the Voigt parameter we include radiative ($C_{\rm rad}$), Stark ($C_{\rm Stk}$), and Van der Waals ($C_{\rm VdW}$) broadening due to hydrogen. For the hydrogen lines, we also include natural broadening. For details on how these mechanisms are considered, see Mauas et al. (1988). For hydrogen, the Stark broadening parameters were computed following Sutton (1978), and those for Van der Waals and natural broadening were computed as in Vernazza et al. (1981). $C_{\rm Stk}$ for the Na D lines and the Ca II K and H lines are from Konjevic et al. (1984), and the $C_{\rm VdW}$ are from Lewis et al. (1972), for the Na D lines and from Monteiro et al. (1988), for Ca II K and H.

Usually, collisions with hydrogen atoms are neglected in the statistical equilibrium equation, due to the larger mass, and therefore smaller velocity of hydrogen atoms with respect to electrons. However, in these cool stars, where the electron density is very low, they might play an important role, in particular around the temperature minimum. Due to the complete lack of reliable atomic data regarding the collision rates with hydrogen, we did not include these rates in our treatment. Furthermore, Andretta et al. (1997) did include them in their calculation of Na I D profiles in dM stars, and found that the effect of these collisions is not important for the emerging profiles of the Na I D lines.

Since the atomic species mentioned above were computed outside of LTE, all opacities, at all the frequencies needed to compute a transition rate, are computed using the actual populations of these species, and the computed values of their population densities are used to compute the electron density and the hydrostatic equilibrium (see Sect. 3.1).

Due to the presence of numerous spectral lines, both atomic and molecular, it is very important to include in the opacity calculations the contribution of this bound-bound absorption, generally referred to as *line blanketing* (see Paper I, Andretta et al., 1997, Short & Doyle, 1997). In this work we included the 58×10^6 atomic and molecular lines computed by Kurucz (1991). Further details on how this opacity is treated is given in Sect. 3.2.

Partial redistribution was included self-consistently for Ly-α and the Mg I fundamental line, for which the Complete Redistribution approximation has demonstrated to be inadequate (Woods et al. 1995, Hubeny & Lites 1995, Mauas et al. 1988, see Sect. 3.3).

We used a microturbulent velocity distribution, matching the distribution in the standard solar model from Vernazza et al. (1981), between 1 and 2 km s$^{-1,}$ both in the hydrostatic equilibrium equation and for the line-profile calculations. Although this is a rather arbitrary choice, the values are similar to the ones given by Giampapa et al. (1982), Houdebine and Doyle (1994a,b) and Andretta et al. (1997). Short & Doyle (1997), used larger values, following Eriksson et al. (1983). However, as this last work refers to giant stars, we prefer the usual values for dwarf stars. Changing the turbulent velocity should have two effects: it affects the hydrostatic equilibrium and therefore the relation between column mass and height, and it increases the Doppler width of the lines. This last effect should be negligible, since we have used broad lines, where the other broadening mechanisms are much more important than the Doppler effect.

To assess the importance of the different approximations, we used two atmospheric models, discussed in Papers I and III: the model for the active star AD Leo, and the one for the very inactive star Gl 588. From now on, we will refer to these models as our "hot" and "cold" model, respectively. The temperature distributions for both models are shown in Fig. 1 as a function of height above the point where $\tau(5000\,\text{Å}) = 1$.

We point out the fact that we have used, as our independent variable, physical depth and not column mass. Therefore, when introducing the different assumptions, we keep constant the temperature (and turbulent velocity) at a given height. If any assumption changes the density in certain points, this can affect

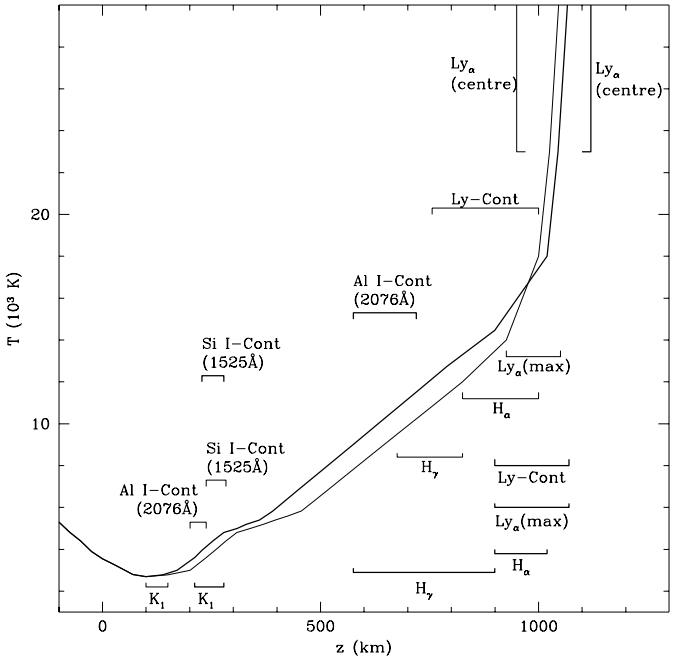

Fig. 1. Temperature distribution for our chromospheric models; the approximate depths where the various continua and lines originate are indicated. Thin line: cold model. Thick line: hot model.

the relationship between height and column mass, in the same way as changing the turbulent velocity.

3. The assumptions

3.1. Metals in LTE

An assumption usually made to simplify the modelling process, is to consider that all the minority species not explicitly considered for the emergent line spectrum, are in Local Thermodynamic Equilibrium (LTE), i.e., that their level populations are described by the Saha and Boltzmann equations.

In other words, if only the continuum and/or the hydrogen lines are used as spectral diagnostics, the only species computed outside LTE is hydrogen. If some other spectral line is also considered, then this species is computed outside of LTE and the others are still assumed in LTE.

In our models we consistently compute the full non-LTE set of equations for He I, He II, C, Fe, Si, Al, Ca, Na and Mg, in addition to H itself, for all the atomic levels indicated in Sect. 2. The contribution to the general opacity from other levels of these species as well as of other species is computed in LTE as explained in Sect. 3.2.

To check the importance that this assumption has on the emergent spectrum, we made a run assuming LTE for the metals mentioned above. In Fig. 2 we show the resulting continuum spectra for our models computed with the metals in LTE (thin line) and in NLTE (thick line). We show only the region below 2800 Å, since above this wavelength the spectra are unchanged.

Note that in the NLTE calculations our cold and hot models have the same predicted continuum above 3500 Å, since the photosphere is the same, while some differences are present below 3500 Å, due to the different contribution of the hot and cold chromosphere to the emission.

In the left panels of Fig. 2, we show the spectra between 100 and 1000 Å. We see that, when LTE is assumed, there is a much stronger emission, up to 3 orders of magnitude. Emission in this region is due to He II, and the larger emission arises from overestimating the He III population when LTE is assumed, in as much as 4 orders of magnitude.

In the right panels of Fig. 2, we show the spectra between 1000 and 2800 Å. Between 1000 and 1200 Å the emission is due to C I continua. Between 1500 and 2800 Å, the continua contributing to the emission are those of Si I ($\lambda \leq 1525$ Å), Mg I ($\lambda \leq 1621$ Å), Si I ($\lambda \leq 1682$ Å), Al I ($\lambda \leq 2076$ Å) and Mg I ($\lambda \leq 2514$ Å). When these metals are treated in LTE, the emission is over or underestimated by as much as a factor of two, for both models, depending on wavelengths. This confirms the results of Short & Doyle (1997), who estimated the changes in the continuum by interpolating the solar departure coefficients.

Computing the metals in LTE also underestimates the electron density in the low chromosphere by as much as a factor of three. However, this difference does not affect the line profiles we studied.

3.2. Line blanketing

Most of the chromospheric models computed up to now, neglected the line blanketing due to the numerous atomic and molecular lines present in the stellar atmosphere. However, we have already pointed out in Paper I that, for active stars, the continuum levels computed with and without line blanketing are very different and therefore result in very different values for the colors of the star. In Paper III we confirmed these results for low activity stars.

Only recently, Andretta et al. (1997) included line blanketing at photospheric levels, and Short & Doyle (1997) included it also at chromospheric levels and examined the dependence of computed line profiles on background opacities.

We briefly explain how these opacities are included in all our models. A more detailed explanation can be found in Avrett et al. (1986). Kurucz's opacities were computed assuming LTE, and are given for 35093 wavelength points in the range 89.7 to 100000 Å, for 56 values of temperature, 21 values of pressure and 5 values of velocity. To reduce the number of wavelength points, every 100 of Kurucz's points are ordered from lower to higher opacity, and the 10th, 30th, 50th, 70th and 90th values are chosen. These five values are assigned to frequencies uniformly distributed over the original interval, but in the order they occurred in the original sample. In this way we replace every 100 of Kurucz's points with only five frequencies. This process is done independently for *each* depth point, and at *each* iteration. In this way, we avoid associating large (or small) opacities for a given frequency to all depths, which is a disadvantage of the use of distribution functions (Carbon 1984).

On the other hand, the source function corresponding to these opacities cannot be assumed equal to the Planck function,

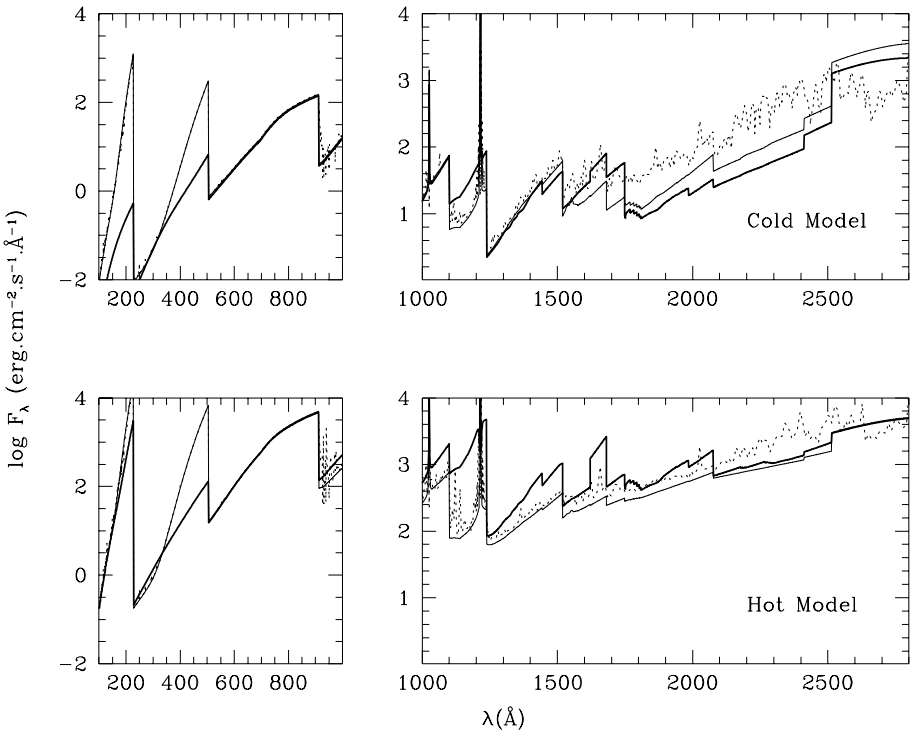

Fig. 2. Continuum flux computed for our atmospheric models. cold model (upper panels) and hot model (lower panels). Thick line: metals in NLTE, without line blanketing. Thin line: metals in LTE, without line blanketing. Dotted line: metals in LTE, with line blanketing

since the blanketing lines are not in LTE in the chromosphere. Therefore, we use a scattering albedo, and compute the source function S_ν as

$$S_\nu = \alpha\, J_\nu + (1-\alpha)\, B_\nu \ , \qquad (3)$$

where B_ν is the Planck function, J_ν is the mean intensity, and α is the scattering albedo, for which we use the expression given by Anderson (1989).

This problem is particularly important in the ultraviolet, since the UV lines are formed in the chromosphere, where assuming LTE would imply very strong emission lines. In Fig. 2 we show the continuum below 3000 Å, for both our models, computed with (dotted line) and without (thin full line) the line blanketing. It can be seen that, even when the scattering albedo is used, the numerous lines contribute to the emission level, notably for the cold model, resulting in a stronger emission. If expression (3) is not taken into account, the contribution of the lines would be much stronger.

This effect is different to what happens in the visible, as can be seen in Fig. 3, since the radiation at these wavelengths comes from the photosphere, and therefore enhancing the opacity implies lower emission levels.

In fact, increasing the opacity moves outwards the region of formation of the radiation. For the part of the spectrum formed in the chromosphere, this implies that the radiation originates where the temperature is larger, and this increases the J_ν value. Instead, for the part of the spectrum formed in the photosphere, an increased opacity implies that the emission originates in layers with lower temperature, due to the opposite sign of the temperature gradient in these two regions of the atmosphere.

We point out the main differences between our calculations of the line blanketing and those by the Armagh group: on one hand, they use a larger line set including, in addition to Kurucz's lines, some triatomic molecules not included in our opacities. Kurucz (1991) himself cautioned against the use of his opacities to compute the atmosphere of M stars, due to the non-inclusion of triatomic molecules in his set. However, based on our results (see Fig. 3) we believe this compilation is good enough even for these stars, as far as a perfect fit of particular features is not expected.

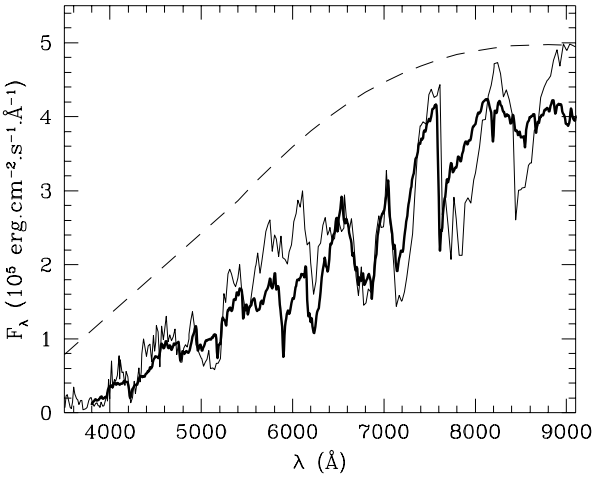

Fig. 3. Continuum intensity in the visible, computed including Kurucz's opacities (full line), and not including them (dashed line). Also shown is the observed spectrum for Gl 588 (thick line).

On the other hand, in our case the line opacities and continuum source functions are included self-consistently at all frequencies used in the calculations, for all lines and continua of all the atomic species computed, and at all depths. This process

is repeated at each iteration, and the new values of pressure are used each time, while Short & Doyle (1997) precomputed the opacities using a different program, and included them only in the continua and in the Ly_α, H_α and P_β lines.

In Fig. 3 we compare the observed spectrum for Gl 588 and the continuum emission computed from our models with and without this opacity source. We point out that the continuum emission is the same for both our models, since the photospheric structure is the same. It can be seen that not including line blanketing results in a much larger continuum intensity. In Papers I and III we showed that the fluxes for the U, B, V, R filters obtained with and without line-blanketing differ strongly, both for active and quiet stars.

When line blanketing is ignored, the region of formation of the continuum moves downwards. In particular, the point where $\tau(5000\,\text{Å}) = 1$ lies deeper in the atmosphere, and therefore the relationship between height and column mass is altered.

For the chromospheric modelling, an accurate continuum level is important in two different ways. It is necessary for a correct comparison between the computed and observed profiles, and it can also affect the statistical equilibrium of the species, and therefore modify the source function of the other lines under consideration. For this reason, we considered line-blanketing in all the transitions we computed, even if the profiles were not to be compared with the observations.

In Fig. 4, as an example, we compare the H_α and H_γ profiles, computed with and without Kurucz opacities, for our cold and hot models. It can be seen in Fig. 4a that, for the cold model there is not only a difference in the value of the continuum, as expected, but also a remarkable difference in the central intensity, (of more than 20% for H_α and more than 70% for H_γ). For the hot model, on the other hand, there is a remarkable difference in the continuum, while the difference in the central intensities is small. Therefore, neglecting line blanketing affects the line profiles in a way that cannot be predicted *a priori*, since it depends on the structure of the particular atmosphere. This holds in general for all the lines. In particular, when we neglect the line blanketing, the central intensity of Ca II H and K line decreases and the Na D lines become narrower for both models.

Often, when comparing the computed and observed profiles, the line profiles relative to the continuum are considered, as are shown in Fig. 4b. We see in Fig. 4a that the two H_α profiles for our hot model differ only in the line wings, when the profiles are compared relative to the computed continuum, however, the differences seem much larger. Conversely, the H_α profiles for our cold model in Fig. 4a are completely different, but can be considered quite similar if the relative intensities are compared, as it is done in Fig. 4b.

The error introduced when relative intensities are considered is larger when the modeling is not based on the profiles, but on some integrated quantities like, for example, equivalent widths or line fluxes, since the error in the computed continuum propagates to these quantities. For the modelling it is important to compare the absolute profiles, whenever the calibration is available.

As an example, in Table 1 we list the integrated flux, the flux with the continuum intensity subtracted, the continuum flux, and the equivalent width for H_α and H_γ, for both our models, computed with and without the line blanketing. It can be seen that, for our cold model, there is a strong change in the line flux, but the equivalent width does not change, since the continuum level is also strongly affected. On the other hand, for our hot model the line flux does not change too much, but the equivalent width is a factor of 2 larger when line blanketing is considered, due to the different level of the continuum.

Therefore, the inclusion of a proper set of opacities is very important for the modelling of the chromosphere, at least at the frequencies of the lines under study. However, when studying a subordinate line it could be necessary to properly include the opacities in all the lines which are important to populate or depopulate the levels involved in the transition.

Even if the right photospheric model is chosen, for example from the grids by Mould (1976), Brett (1995) or Allard and Hauschildt (1995), and the line blanketing is included for all transitions, comparison between the observed and computed profiles is very difficult, since there is no way to guarantee that the continuum intensity is correct at every wavelength. In this paper, and in our former work, because the total opacities given by Kurucz do not always match the observed spectrum, for each line we study in detail, we modify the background opacities until the computed and observed continuum intensity coincide.

3.3. The Lyman-α line in Complete Redistribution

The Ly_α flux has often been used as an atmospheric diagnostics. In particular, the Armagh group has used the ratio of the Ly_α to the H_α flux to constrain the position and the structure of the transition region (Houdebine & Doyle 1994a; Houdebine et al. 1995; see also Doyle et al. 1997). However, they have treated the Ly_α source function using the Complete Frequency Redistribution (CRD) approximation, which is known to be rather poor for resonance lines, and in particular for Ly_α (e.g. see Vernazza et al. 1981; Hubeny & Lites 1995).

For our models, we have computed Ly_α with a Partial Redistribution (PRD) treatment, following Vernazza et al. (1981; see their Appendix A for details). In this method, the probability for coherent scattering in the line wings is given by

$$\gamma_s = \frac{\Gamma_{\rm rad}}{\Gamma_{\rm rad} + \Gamma_{\rm E}} \,, \tag{4}$$

where $\Gamma_{\rm rad}$ and $\Gamma_{\rm E}$ are the radiative and collisional damping coefficients, for which the scattering in the line is expected to be coherent and non-coherent, respectively (we have not set any limits on γ_s, as has been done by Vernazza et al. 1981).

In this treatment there is a free parameter, the frequency which separates the CRD Doppler core, and the line wings, where scattering is completely coherent. In our calculations we have taken this frequency to be equal to the Doppler width, which gives the best match both for the AD Leo Ly_α flux (see Paper I), and for the observed ratio of the Ly_α to the H_α flux. If this parameter is changed, not only the Ly_α flux will be different,

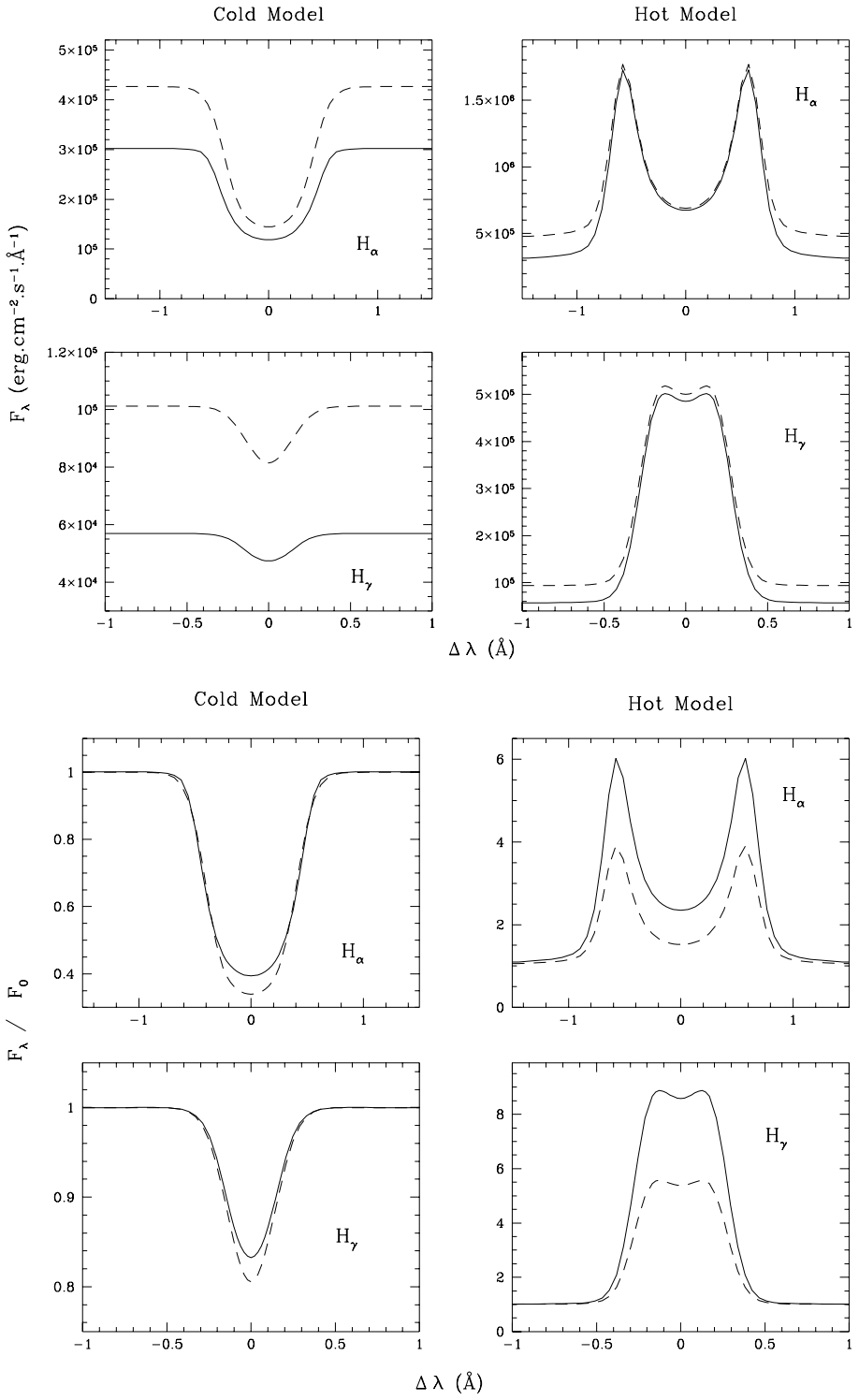

Fig. 4a and b. H_α and H_γ profiles computed with (full line), and without (dashed line) Kurucz's opacities. **a** Absolute intensities; **b** Relative intensities.

but the statistical equilibrium of hydrogen will be affected, and therefore the line profiles of the other hydrogen lines can be different.

To check the effects of the CRD assumption, we also made computations assuming CRD, for both our models. In Fig. 5 we compare the Ly_α profiles obtained with the CRD assumption with the ones computed in PRD.

For the cold model, the differences in the line core emission computed with the two methods are much larger than for the Sun. This is due to two factors: first, due to a smaller density in the region where the Ly_α peak is formed $\Gamma_{\rm E}$ is smaller, and γ_s in Eq. (4) is larger. In other words, Partial Redistribution effects are more important than for the Sun, since coherent scattering is more likely to occur because collisions are less frequent.

Table 1. Line parameters for our cold (C) and hot (H) models: the flux integrated over the line F (erg cm^{-2} s^{-}1), the flux with the continuum subtracted, integrated over the line F_o (erg cm^{-2} s^{-1}), the continuum flux near line center F_c (erg cm^{-2} s^{-1} Å^{-1}), and the Equivalent Width (Å).

Model	line	F	F_o	F_c	W_{eq}
C	H_α	$7.5\ 10^7$	$-1.5\ 10^5$	$3.0\ 10^5$	0.51
	H_γ	$9.4\ 10^6$	$-3.3\ 10^3$	$5.7\ 10^4$	0.06
C (no blanketing)	H_α	$1.1\ 10^8$	$-2.3\ 10^5$	$4.3\ 10^5$	0.54
	H_γ	$1.7\ 10^7$	$-6.8\ 10^3$	$1.0\ 10^5$	0.07
H	H_α	$1.1\ 10^8$	$1.4\ 10^6$	$2.9\ 10^5$	-4.8
	H_γ	$1.5\ 10^7$	$2.7\ 10^5$	$5.7\ 10^4$	-4.7
H (no blanketing)	H_α	$1.2\ 10^8$	$1.2\ 10^6$	$4.5\ 10^5$	-2.6
	H_γ	$1.6\ 10^7$	$2.5\ 10^5$	$9.3\ 10^4$	-2.7

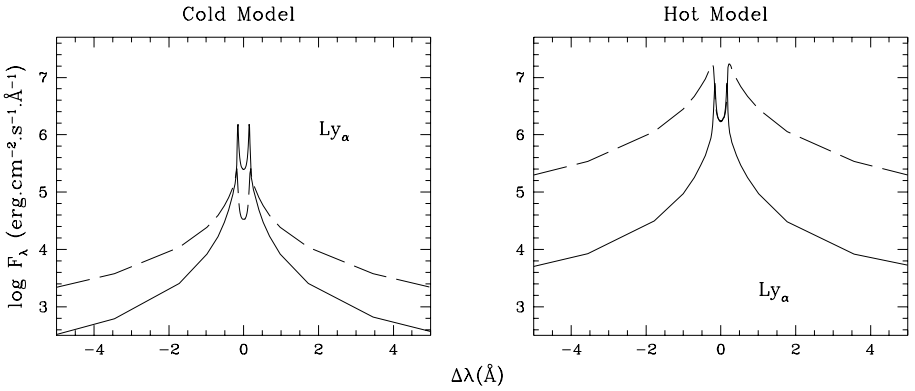

Fig. 5. Ly$_\alpha$ computed profiles for our cold (left panel) and hot (right panel) models. Full line: PRD profile; Dashed line: CRD profile.

On the other hand, for this cold model there is not a well differentiated region of formation for the Ly$_\alpha$ peak and the H$_\alpha$ line core, as occurs in the Sun. Therefore, a change in the statistical equilibrium equation, an effect that can be considered of second order in the Sun (see Hubeny & Lites 1995), strongly affects the Balmer line profiles. In Fig. 6 (left panels) we show the H$_\alpha$ and H$_\gamma$ profiles for this model obtained when Ly$_\alpha$ is computed in CRD and in PRD.

In fact, we see in Fig. 1 that the layers of formation of the H$_\alpha$ line centre overlap with those of the Ly$_\alpha$ maximum (this result has been reported by Houdebine & Doyle 1994, for dMe stars). Therefore, a change in the Ly$_\alpha$ profile of the magnitude shown in Fig. 5 when CRD is assumed, reduces the $\int J_\nu \phi_\nu d\nu$ for Ly$_\alpha$, by an order of magnitude. This, through the statistical equilibrium equation, implies a population for level 2 around 30 times lower in the high chromosphere. Therefore, the opacity in the Balmer lines is much smaller, and the region of formation of these lines moves down to a broad region between 300 and 800 km, to be compared with the one shown in Fig. 1. Then, when CRD is assumed, the layers where the Balmer lines originate have lower temperature and microturbulent velocity and the absorption lines are narrower compared with the ones obtained when PRD is taken into account.

The changes in the statistical equilibrium equation due to changes of $\int J_\nu \phi_\nu d\nu$ for Ly$_\alpha$, can also affect the ionization equilibrium of hydrogen. In particular, for our cold model the electron density computed with Ly$_\alpha$ in CRD is almost an order of magnitude smaller in the high-chromosphere. Such a change of electron density produces a variation in the gas pressure, which in turn affects the relationship between height and column mass. When CRD is assumed, the column mass of the transition region is smaller.

For our hot model, the Ly$_\alpha$ profiles are shown in Fig. 5 (right panels) and the H$_\alpha$ and H$_\gamma$ profiles in Fig. 6 (right panels). We can see that in this case the Ly$_\alpha$ line centre remains unchanged. Therefore, the $\int J_\nu \phi_\nu d\nu$ changes very little, and the level 2 population is only 30% smaller in the CRD case. For this reason, the Balmer lines originate in the same regions for both treatments, and changes in the line profiles are only due to the changes in the source functions.

We have already pointed out that the Ly$_\alpha$ to H$_\alpha$ flux-ratio has been used as a diagnostics for atmospheric modelling. However, assuming CRD for Ly$_\alpha$ modifies this ratio as little as 10%, for our hot model, or as much as a factor of 5, for our cold model.

We also performed a calculation with the Ly$_\beta$ line computed in PRD, and found that there where no changes in the profiles or the electron densities. This fact implies that, for both models, this line can be safely computed in CRD, which confirms the results obtained by Hubeny & Lites (1995) for the Sun.

For our cold model the assumption of CRD for Ly$_\alpha$ implies a variation of electron density with respect to the one obtained when PRD is taken into account (see Sect. 3.3.1). This change of electron density in the high chromosphere can affect the emergent profiles of the lines which originate in these layers. In

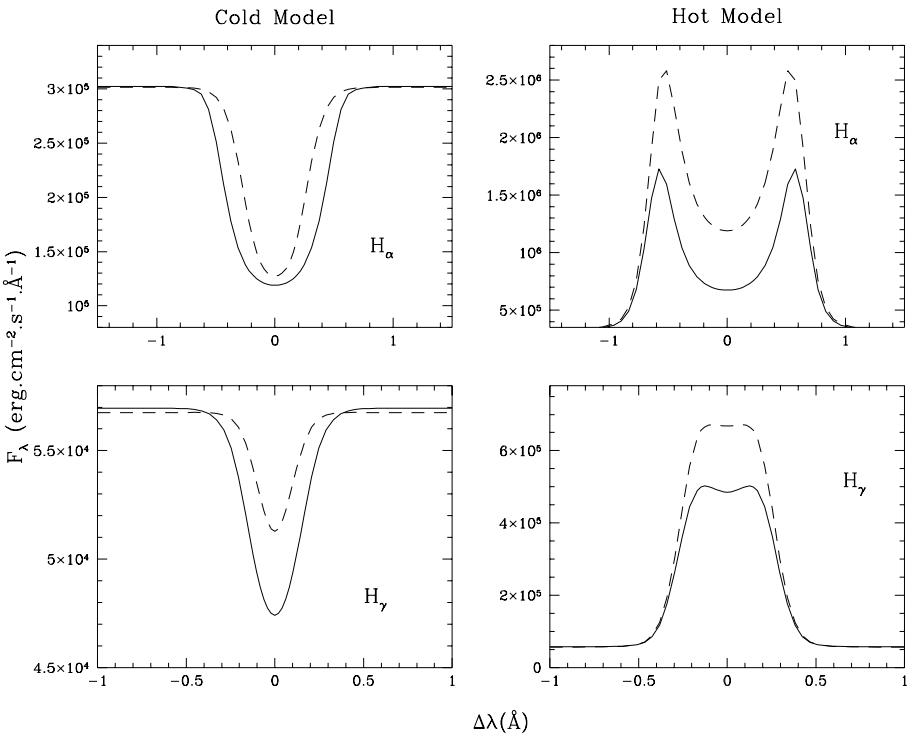

Fig. 6. H_α and H_γ computed profiles for our cold (left panel) and hot (right panel) models. Full line: profiles computed when Ly_α is treated with PRD; Dashed line: profiles computed when Ly_α is treated with CRD.

particular, the Ca II H and K lines may be suitable to investigate this effect, because they are collision-dominated lines and tend to couple with local conditions. Therefore, we computed the calcium lines for our cold model (defined when Ly_α is computed in PRD) and for the model obtained when the Ly_α line is computed in CRD. In both cases, the H and K lines are treated in PRD. As an example, we show in Fig. 7a the effects of the model changes on Ca II K line profile: it can be seen that the resulting profiles are very different in the emission core. A central reversal is present when Ly_α is computed in the CRD approximation, due to the fact that the lower electron density allows the source function to drop much faster. The wings and in particular the K_1 minimum, are not strongly affected, since they are formed in a region where the source function is still strongly coupled to the Planck function.

On the other hand, the H and K lines are resonance lines which are known to be affected by PRD effects. To study the effect of the CRD assumption for these lines we computed them in the CRD approximation for the model obtained when the Ly_α line is computed in CRD. The obtained K line profile is shown in Fig. 7b (dotted line) and compared with the one computed with PRD for the same model. As expected the PRD (dashed line) and CRD profiles are very similar in the emission core and differ in the wings. In particular, the CRD assumption for the K line strongly affects the intensity of the K_1 minimum. Therefore, if the K_1 minimum is used as diagnostics for the structure of the T_{min} region in atmospheric modelling (Mauas & Falchi 1998), it is important to compute the K line in PRD.

For our hot model assuming CRD for Ly_α affects very little the electron density, and therefore there are no variations in the Ca II H and K profiles.

4. Conclusions

We studied how different approximations, usually made to simplify the computation of chromospheric models, can affect the computed spectrum emitted by two atmospheric models: a cold one, corresponding to the low-activity dM star Gl 588, and a hot one, corresponding to the very active star AD Leo.

We found that assuming that the minority species are in LTE leads to underestimate the electron density in the low chromosphere, and changes the continuum emission for $\lambda \leq 2600$ Å. On the other hand, this assumption does not affect the profile of the hydrogen lines, or those of Ca II K and Na D. Therefore, if only these profiles are to be used as a modelling tool, there is no need to compute self-consistently the NLTE population of the metals.

To neglect line blanketing when computing the background opacities, affects strongly not only the computed continuum, as expected, but also affects the population balance between different levels of the atomic species under consideration, and therefore the computed line-centre intensities. The continuum intensity effect is often neglected and the line profiles, relative to the continuum, are studied; we show that it is not enough, since also in this case the computed profiles are very different.

We study how assuming complete frequency redistribution in the Ly_α line affects the computed profiles. We see that the profile differs much strongly than in the solar case, due mainly to the fact that the region of formation is the same for H_α and Ly_α, and therefore the statistical equilibrium equation of hydrogen is strongly affected when Ly_α is computed in CRD.

The effect of the CRD assumption is much stronger for our cold model than for our hot one, due in part to the lower electron densities. For the cold model, in CRD the second level of

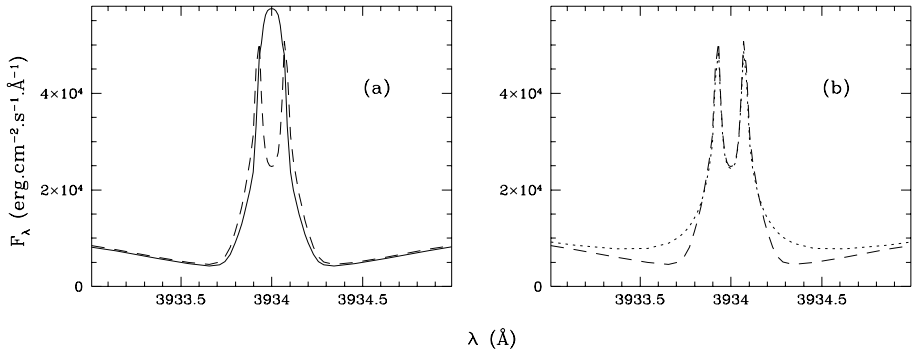

Fig. 7a and b. Ca II K line profiles for our Cold model. **a** computed in PRD, when Ly_α is computed in PRD (full line), and in CRD (dashed line). **b** computed in CRD (dotted line) and in PRD (dashed line) when Ly_α is computed in CRD

hydrogen is underpopulated, and the Balmer lines form deeper in the atmosphere. Also, in this case, CRD implies an underionization of hydrogen, and therefore lower electron densities than in PRD. This, in turn, affects other lines formed in the chromosphere, like the Ca II H and K lines, which are frequently used as atmospheric diagnostics.

When modelling stellar atmospheres, the line profiles are usually matched to a much larger precision than the changes produced in the computed profiles by assuming CRD or neglecting line-blanketing (see Mauas & Falchi 1998). Therefore, we believe that it is very important to carry on a complete modelling process, free of these approximations, if useful conclusions on the chromospheric structure are to be drawn.

Acknowledgements. We would like to thank the referee, Dr. R. Robinson, for constructive criticisms that helped to improve the paper.

References

Allard F., Hauschildt P.H., 1995, ApJ, 445, 433
Anderson L.S., 1989, ApJ, 339, 558
Andretta V., Doyle J.G., Byrne P.B., 1997, A&A, 322, 266
Avrett E.H., Loeser R., 1984, in "Methods in Radiative Transfer", (W. Kalkofen ed.) Cambridge, Univ. Press, p. 341.
Avrett E.H., Machado M.E., Kurucz R.L., 1986, in "The Lower Atmosphere of Solar Flares" (D.F. Neidig, ed.) NSO Summer Workshop, Sunspot, New Mexico, 216
Brett J.M., 1995, A&A, 295, 736
Carbon D.F. 1984, in " Methods of radiative transfer" (W. Kalkofen ed.) 395
Cram L.E., Mullan D.J., 1979, ApJ, 234, 579
Doyle J.G., Mathioudakis M., Andretta V., Short C.I., Jelinski, P. 1997, A&A 318, 853
Eriksson K., Linsky J.L., Simon, T. 1983, ApJ, 272, 665
Giampapa M.S., Worden S.P., Linsky, J.L., 1982, ApJ, 258, 740
Houdebine E.R., Doyle J.G. 1994a, A&A, 289, 169
Houdebine E.R., Doyle J.G. 1994b, A&A, 289, 185
Houdebine E.R., Doyle J.G., Kościelecki M., 1995, A&A, 294, 773
Houdebine E.R., Mathioudakis M., Doyle J.G., Foing B.H., 1996, A&A, 305, 209
Hubeny I., Lites B.W. 1995, ApJ, 455, 376
Konjevic N., Dimitrijevic M., Swiese W.L., 1984, J. Phys. Chem. Ref. Data 13, 649
Kurucz R.L., 1991, in: Precision Photometry: Astrophysics of the Galaxy, eds. A.G. Davis Philip, A.R. Upgren, and K.A. Janes, L. Davis Press, Schenectady
Lewis E.L., McNamara L.F., Michels H.H., 1972, Sol. Phys. 23, 287
Luttermoser D.G., Johnson H.R., Eaton J. 1994, ApJ, 422, 351
Mauas P.J., Avrett E.H., Loeser R. 1988, ApJ, 330, 1008
Mauas P.J., Falchi, A. 1994, A&A, 281, 129 (Paper I)
Mauas P.J., Falchi, A. 1996, A&A, 310, 245 (Paper II)
Mauas P.J., Falchi, A., Pasquini, L., Pallavicini, R. 1997, A&A 326,249 (Paper III)
Mauas P.J., Falchi, A. 1998, A&A, in preparation.
Monteiro T.S., Danby E.L., Cooper I.L., Dickinson A.S., Lewis E.L., 1988, J.Phys.B 21, 4165
Mould J.R., 1976, A&A, 48, 443
Robinson, R.D., Cram L.E., Giampapa M.S., 1990, ApJS 78, 891
Short C.I., Doyle J.G. 1997, A&A 326,287
Sutton K., 1978, JQSRT 20, 233
Thatcher J.D., Robinson R.D., Rees D.E., 1991, MNRAS 250, 14
Tripicchio A., Severino G., Covino E., Terranegra L., García López J., 1997, A&A 327, 681
Vernazza, J.E., Avrett E.H., Loeser R. 1981, ApJS 45, 635
Woods T.N., Rottman G.J., White O.R., Fontenla J., Avrett E.H., 1995, ApJ, 442, 898